Nonstandard finite differences numerical methods for a vegetation reaction-diffusion model

Dajana Conte[a], Giovanni Pagano[a], Beatrice Paternoster[a]

[a]*Department of Mathematics, University of Salerno, Fisciano, Italy. E-mail: {dajconte,gpagano,beapat}@unisa.it*

Abstract

In this work we derive NonStandard Finite Differences (NSFDs) [1, 35] numerical schemes to solve a model consisting of reaction-diffusion Partial Differential Equations (PDEs) that describes the coexistence of plant species in arid environments [21]. The new methods are constructed by exploiting a-priori known properties of the exact solution, such as positivity and oscillating behavior in space. Furthermore, we extend the definition of NSFDs inspired by the Time-Accurate and High-Stable Explicit (TASE) methodology [2], also exploring the existing connections between nonstandard methods and the Exponential-Fitting (EF) [28, 29] technique.

Several numerical tests are performed to highlight the best properties of the new NSFDs methods compared to the related standard ones. In fact, at the same cost, the former are much more stable than the latter, and unlike them preserve all the most important features of the model.

Keywords: Nonstandard finite differences, exponential fitting, TASE technique, stable numerical methods, reaction-diffusion partial differential equations.

1. Introduction

Models of differential equations that represent chemical, physical, biological and other types of phenomena are increasingly frequent in the scientific literature. Providing analytical solutions of such models is not often possible, and therefore the use of numerical methods becomes necessary. Furthermore, it may happen that qualitative characteristics of the exact solution of the analyzed model are a-priori known. For example, epidemiological models [8, 22, 23, 46] that represent the evolution over time of quantities of individuals cannot produce negative solutions. Or, chemical models that represent reactions that are periodically in a given state [5, 6, 7] must produce oscillating solutions. Therefore, the choice of the method must be weighted, as there is a risk, otherwise, of calculating an uncoherent numerical solution for the considered model.

In this paper, we focus on the numerical solution of a reaction-diffusion Partial Differential Equation (PDE) model [21] describing the evolution of vegetation in arid environments, building new explicit and stable methods able to preserve all its main features. The mentioned PDE system is the following:

$$\begin{cases} \dfrac{\partial u_1}{\partial t} = \dfrac{\partial^2 u_1}{\partial x^2} + w u_1(u_1 + H u_2) - B_1 u_1 - S u_1 u_2, \\ \dfrac{\partial u_2}{\partial t} = D\dfrac{\partial^2 u_2}{\partial x^2} + G w u_2(u_1 + H u_2) - B_2 u_2, \\ \dfrac{\partial w}{\partial t} = d\dfrac{\partial^2 w}{\partial x^2} + A - w - w(u_1 + u_2)(u_1 + H u_2), \end{cases} \qquad (x,t) \in \Omega := [x_0, X] \times [t_0, T]. \qquad (1.1)$$

Here, A, B_1, B_2, d, D, G, H and S are positive parameters.

The functions u_1 and u_2 represent the density of two different types of plants. For example, u_1 can indicate a grass species and u_2 a tree species. Finally, w is the amount of water available at a given time and spatial point of the domain. This model allows to understand how the coexistence of both species occurs as the amount of water varies. It can be proved [21] that coexistence is only a transient solution of the system, since after a considerable period of time one between u_1 and u_2 goes to zero. Therefore, coexistence can be regarded as a metastable solution. Trivially, all the functions of the system are non-negative at each point of the domain. Moreover, as long as the two species coexist, u_1, u_2 and w oscillate in space with constant frequency [21]. Hence, we are interested in developing numerical methods which preserve these characteristics and of course the metastability.

To build the new methods, we combine NonStandard Finite Differences (NSFDs) [1, 35] and Time-Accurate and High-Stable Explicit (TASE) [2, 9] techniques. The latter can be applied to improve the stability properties of numerical methods. The NSFDs are usually used to make the numerical solution able to preserve the main properties of the exact one. There is a close connection between these two techniques, and in fact in this paper we give an extended definition of NSFDs inspired by TASE methodology, showing that in this way we obtain nonstandard methods with excellent stability properties.

The TASE technique [2, 9] has been recently introduced. It leads to improving the stability properties of explicit numerical methods through an appropriate modification of the differential problem to solve. The NSFDs, on the other hand, are an alternative technique to Standard Finite Differences (SFDs) for the discretization of differential equations. They consist in modifying the coefficients of explicit SFDs methods in order to adapt them to the considered model and its known properties [1, 35]. The fundamental thing is that NSFDs methods are still explicit, and therefore they do not involve significant additional computational costs compared to the related SFDs schemes. Most of the existing work in the literature on NSFDs [15, 31, 40, 41] is aimed at preserving the positivity [10, 34] and equilibrium points properties [38, 39] of a physical system. In this paper, we show that it is also possible to preserve the oscillating trend, if any, of the solution of a model by incorporating the Exponential-Fitting (EF) technique into the NSFDs.

Indeed, the EF technique [28, 29] allows to construct highly accurate numerical methods for differential problems having oscillating solutions with known constant frequency. The EF consists in fixing a basis of functions, called fitting space, imposing that the numerical solution determined by the considered method is exact on it. This leads to new method coefficients dependent on the oscillation frequency. In the literature, there are several works on EF-based Runge-Kutta [11, 16, 18, 19, 44] and peer [12, 13, 14] methods. The exponentially fitted methods result more accurate than the relative classical ones when the functions of the fitting space well mimic the trend of the solution, and when the oscillation frequency is very high. In this work we assume that the frequency is known, estimating it by means of a reference solution. Several techniques are available from the literature to numerically estimate the frequency related to the solution of some problems when unknown [20, 42, 43]. However, to our knowledge, there are no manuscripts focusing on the application of EF methods with a-priori estimation of the frequency, when the problem to solve consists of non-linear PDEs with oscillating in space solution, like the one analyzed there.

Therefore, in this paper, in addition to showing how, starting from an explicit SFDs method, it is possible to construct much more stable NSFDs methods, able to preserve the positivity and oscillations of the considered model, we extend the classic definition of NSFDs inspired by TASE technique, also showing that EF methods can be interpreted as particular nonstandard schemes. Therefore, from now on, the NSFDs can be used both to obtain methods with optimal stability properties, and to preserve

the oscillating trend, if any, of the analyzed problem.

This work is organized as follows. In Section 2 we describe the NSFDs, extending the related definition. In Section 3 we show that the application of the EF technique can be interpreted as a special case of the use of nonstandard discretizations. In Section 4 we apply the extended NSFDs definition to derive stable nonstandard methods for the model (1.1), which are also able to follow its oscillating trend. In Section 5 we further modify the previously derived NSFDs schemes to preserve the positivity of the exact solution. In Section 6 we highlight through numerical tests the advantages of the new proposed NSFDs methods. Finally, in Section 7, we discuss the obtained results and possible future research.

2. Nonstandard finite differences and TASE technique

In this section, we give the definition of NSFDs numerical methods, then extending it inspired by TASE methodology. Let us consider an Ordinary Differential Equation (ODE) system of the following form:

$$\begin{cases} \dfrac{dy}{dt} = F\big(t, y(t)\big), \\ y(t_0) = y_0, \end{cases} \qquad t \in [t_0, T], \quad y : [t_0, T] \to \mathbb{R}^d, \quad F : [t_0, T] \times \mathbb{R}^d \to \mathbb{R}^d. \tag{2.1}$$

To numerically solve this problem, we fix the discrete grid $\{t_n = t_0 + n\Delta t, n = 0, ..., N, t_N = T\}$, then determining approximations y_n of $y(t_n)$ at all mesh points. The simplest classical explicit numerical scheme that can be used for the solution of the ODE system (2.1) is Euler method:

$$y_{n+1} - y_n = \Delta t F(t_n, y_n). \tag{2.2}$$

It is based on the following approximation of the first derivative at $t = t_n$:

$$\frac{dy}{dt}(t_n) \approx \frac{y_{n+1} - y_n}{\Delta t}. \tag{2.3}$$

Starting from classic explicit schemes, it is possible to derive the related NSFDs methods.

Definition 1. *[1, 35] Consider an explicit SFDs numerical method for solving the ODE system* (2.1)*. By making at least one of the following changes, it is possible to obtain a related NSFDs method.*

- *In the approximation of $y'(t)$ at $t = t_n$ in the formula* (2.3)*, the discretization step-size Δt is replaced by a non-negative scalar function $\varphi(\Delta t)$, which approaches Δt when Δt is close to zero, i.e. it holds that $\varphi(\Delta t) = \Delta t + O(\Delta t^2)$, for $\Delta t \to 0$, giving rise to*

$$\frac{dy}{dt}(t_n) \approx \frac{y_{n+1} - y_n}{\varphi(\Delta t)}.$$

- *The function F is non-locally modified, i.e. some of its terms can be reshaped using different grid points. For example, terms such as y^2 can be approximated with $ay_n^2 + (1-a)y_{n+1}y_n$, $a \in \mathbb{R}$, instead of y_n^2.*

For higher order ODEs, standard numerical methods are based on the approximation of order m derivatives by means of SFDs involving the powers Δt^m. In these cases the first property of Definition 1 can be generalized by replacing Δt^m by a non-negative scalar function $\varphi(\Delta t)$, such that $\varphi(\Delta t) = \Delta t^m + O(\Delta t^{m+1})$, for $\Delta t \to 0$. The mentioned properties allow to obtain consistent NSFDs methods with the problem to solve, as we will see in next sections.

Remark 1. *The described approach can be naturally generalized to finite difference methods for PDEs, also discretizing the spatial derivatives of order m by means of NSFDs involving a non-negative scalar function $\phi(\Delta x)$ such that $\phi(\Delta x) = \Delta x^m + O(\Delta x^{m+1})$, for $\Delta x \to 0$, instead of the power Δx^m, where Δx is the discretization step-size in space.*

The NSFDs methods are used to preserve the known features of the analyzed model, such as the positivity or equilibrium points properties. Generally, nonstandard methods are more stable than the relative SFDs schemes. The TASE methodology [2, 9] constitutes an alternative technique that leads to an improvement of the stability of explicit methods. It foresees the numerical solution of the system (2.1) through the following steps.

Firstly, the function F of the system (2.1) is pre-multiplied by a suitably chosen linear operator $T(\Delta t) \in \mathcal{L}(\mathbb{R}^d, \mathbb{R}^d)$ approximating the identity, i.e.

$$T(\Delta t) = I_d + O(\Delta t^p), \text{ for } \Delta t \to 0, \qquad I_d = \text{Identity matrix of order } d, \tag{2.4}$$

thus obtaining the modified ODE system

$$\begin{cases} \dfrac{du}{dt} = T(\Delta t) F\big(t, u(t)\big), \\ u(t_0) = y_0. \end{cases} \tag{2.5}$$

Property (2.4) guarantees that the exact solution $u(t)$ of the problem (2.5) satisfies for some norm

$$||u(t) - y(t)|| = O(\Delta t^p). \tag{2.6}$$

Subsequently, an explicit method of order p is applied to the modified system (2.5). Appropriate choices of the explicit method and the function $T(\Delta t)$ allow for the construction of highly stable numerical schemes. Furthermore, thanks to the equality (2.6), the numerical solution of the modified problem (2.5) turns out to be an order p approximation of that of the original system (2.1). The overall numerical integration scheme obtained in this way generally involves inversions of matrices dependent on the Jacobian of F at each time step [2, 9].

Note that the idea of TASE technique is similar to that of the NSFDs. In fact, consider for example the following nonstandard Euler method obtained through the first property of Definition 1:

$$y_{n+1} - y_n = \varphi(\Delta t) f(t_n, y_n), \qquad \varphi(\Delta t) = \Delta t + O(\Delta t^2). \tag{2.7}$$

The numerical solution of the original system (2.1) computed by applying the method (2.7) corresponds to the numerical solution of the modified problem (2.5) using

$$T(\Delta t) = \frac{\varphi(\Delta t)}{\Delta t} I_d,$$

by means of explicit Euler (2.2). Observe that $T(\Delta t) = I_d + O(\Delta t)$. Hence, since explicit Euler has order one, the function $T(\Delta t)$ respects the TASE definition. The TASE technique can therefore be seen as an extension of the first property of NSFDs. The difference between the two techniques lies in the fact that NSFDs require the use of a scalar function $\varphi(\Delta t)$, while TASE methodology permits that $T(\Delta t)$ can be a matrix function. Therefore, we now extend the first property of NSFDs to allow the use of non-scalar functions.

Definition 2. *Consider an explicit SFDs numerical method for solving the ODE system* (2.1)*. The related NSFDs scheme can be obtained by applying at least one of the two rules described in Definition 1 or the following one.*

- *In the approximation of* $y'(t)$ *at* $t = t_n$ *in the formula* (2.3)*, the step-size* Δt *is 'replaced' by a positive semi-definite matrix function* $\varphi(\Delta t) \in \mathbb{R}^{d,d}$ *, which approaches* $I_d \Delta t$ *when* Δt *is close to zero, i.e. it holds that* $\varphi(\Delta t) = I_d\big(\Delta t + O(\Delta t^2)\big)$*, for* $\Delta t \to 0$*, giving rise to*

$$\frac{dy}{dt}(t_n) \approx \varphi^{-1}(\Delta t)(y_{n+1} - y_n).$$

Obviously, as for Definition 1, we can generalize Definition 2 to derivatives of order greater than one. In these cases, the powers Δt^m appearing after a standard time discretization can be 'replaced' by positive semi-definite matrix functions satisfying $\varphi(\Delta t) = I_d\big(\Delta t^m + O(\Delta t^{m+1})\big)$, for $\Delta t \to 0$.

Note that the definition just given naturally extends the first property of NSFDs to the multidimensional case. In fact, in the scalar case, $\varphi(\Delta t)$ is a non-negative function that approximates Δt. For our extension, $\varphi(\Delta t)$ can also be a positive semi-definite matrix function that approximates $I_d \Delta t$. In deriving the new methods proposed in this paper, we will use Definition 2 assuming that $\varphi(\Delta t)$ is also symmetric.

3. Nonstandard finite differences and exponential fitting

In this section, we describe the EF technique, showing that it leads to particular NSFDs methods. The connection between EF and NSFDs is important, since thanks to it we can improve the accuracy of nonstandard numerical methods when the solution of the differential problem to solve has an oscillating character.

In the Introduction, we mentioned that the exact solution of the model (1.1) oscillates in space with some frequency. Therefore, the application of the EF technique allows to derive the following very accurate discretization of the spatial second order derivative [17]:

$$\frac{\partial^2 u}{\partial x^2}(x,t) \approx \frac{a_0(z)u(x+\Delta x,t) + a_1(z)u(x,t) + a_2(z)u(x-\Delta x,t)}{\Delta x^2}, \qquad z = \omega \Delta x, \tag{3.8}$$

$$a_0(z) = \frac{-z^2}{2(cos(z)-1)}, \qquad a_1(z) = \frac{z^2}{cos(z)-1}, \qquad a_2(z) = \frac{-z^2}{2(cos(z)-1)}. \tag{3.9}$$

Here, ω is a constant parameter representing the oscillation frequency in space of the exact solution.

The EF coefficients $a_i(z)$, $i = 1, 2, 3$, depend on the oscillation frequency. They are obtained by annihilating the following linear operator on the fitting space $\mathcal{F} = \{1, sin(\omega x), cos(\omega x)\}$:

$$\mathcal{L}u(x,t) = \frac{\partial^2 u}{\partial x^2}(x,t) - \frac{a_0(z)u(x+\Delta x,t) + a_1(z)u(x,t) + a_2(z)u(x-\Delta x,t)}{\Delta x^2}.$$

This means that, considering t as a constant, the operator $\mathcal{L}u(x,t)$ thus defined is equal to zero if $u(x,t)$ is a linear combination of the functions of the fitting space. Therefore, the more the exact solution of the considered model behaves in space like the functions of $\mathcal{F}$, the more the EF technique allows to reduce the error of the spatial second order derivative discretization. It is possible to generalize the EF technique even when the solution is characterized by k frequencies ω_j, $j = 2, ..., k$. However, in this case it is necessary to choose a finite difference formula involving more than three free frequency-dependent coefficients to be determined [28].

We now show that the finite differences obtained by applying the EF technique are NSFDs methods.

Proposition 1. *The exponentially fitted discretization* (3.8) *is an NSFDs discretization.*

Proof. Using classic SFDs of order two, the spatial second order derivative can be discretized as follows:

$$\frac{\partial^2 u}{\partial x^2}(x,t) \approx \frac{u(x+\Delta x,t) - 2u(x,t) + u(x-\Delta x,t)}{\Delta x^2}.$$

According to Definition 1 and Remark 1, the related NSFDs discretization can be derived by replacing Δx^2 with a scalar function $\phi(\Delta x)$ such that $\phi(\Delta x) = \Delta x^2 + O(\Delta x^3)$, for $\Delta x \to 0$. Consider the function

$$\phi(\Delta x) = \frac{2\big(1 - cos(\omega \Delta x)\big)}{\omega^2}, \tag{3.10}$$

where ω is a constant parameter. Obviously, the function $\phi(\Delta x)$ is non-negative. Furthermore, its Taylor series expansion near zero is

$$\phi(\Delta x) = \Delta x^2 - \frac{\omega^2 \Delta x^4}{12} + \frac{\omega^4 \Delta x^6}{360} - \frac{\omega^6 \Delta x^8}{20160} + O(\Delta x^{10}) = \Delta x^2 + O(\Delta x^4). \tag{3.11}$$

Therefore, the following constitute an NSFDs discretization for the spatial second order derivative:

$$\frac{\partial^2 u}{\partial x^2}(x,t) \approx \frac{u(x+\Delta x,t) - 2u(x,t) + u(x-\Delta x,t)}{\phi(\Delta x)}.$$

Observe that it exactly corresponds to the exponentially fitted discretization (3.8), with $z = \omega \Delta x$. Therefore, the proposition is proved. □

The proof just provided allows to conclude that the exponentially fitted discretization obtained by applying the EF on the fitting space $\mathcal{F} = \{1, sin(\omega x), cos(\omega x)\}$ is a nonstandard discretization. Considering different basis functions in $\mathcal{F}$, which can be found in the paper [28], leads to new exponentially fitted discretizations which are always nonstandard discretizations. To prove this, it is sufficient to make similar steps to those of Proposition 1.

4. Stable nonstandard numerical methods for the considered model

In this section, we derive two nonstandard methods to solve the model (1.1) by applying the EF in the spatial semi-discretization as shown in Section 3 and an NSFDs scheme in time by following Definition 2. We prove that such methods have much better stability properties than the related standard one.

4.1. Introductory concepts and initial standard discretization

Consider the Dahlquist test equation

$$y'(t) = \lambda y(t), \qquad \lambda \in \mathbb{C}, \quad Re(\lambda) \leq 0, \quad t \in [t_0, T],$$

and the following numerical methods for its solution:

$$y_{n+1} - y_n = \gamma_1(\Delta t)\lambda y_n, \qquad \gamma_1(\Delta t) = \frac{e^{\lambda \Delta t} - 1}{\lambda}, \tag{4.1}$$

$$y_{n+1} - y_n = \gamma_2(\Delta t)\lambda y_n, \qquad \gamma_2(\Delta t) = \frac{\Delta t}{1 - \lambda \Delta t}. \tag{4.2}$$

The Taylor series expansion of the introduced functions $\gamma_1(\Delta t)$ and $\gamma_2(\Delta t)$ is, respectively

$$\gamma_1(\Delta t) = \Delta t + \frac{\lambda \Delta t^2}{2!} + O(\Delta t^3), \qquad \gamma_2(\Delta t) = \Delta t + \lambda \Delta t^2 + O(\Delta t^3). \tag{4.3}$$

Doing simple calculations, note that the first considered numerical method (4.1) is exponential Euler [25] for scalar problems, while the second (4.2) is implicit Euler. These two numerical methods have excellent stability properties with respect to the SFDs scheme associated with them, that is explicit Euler. Hence, the use of the functions $\gamma_i(\Delta t)$, $i = 1, 2$, thus defined instead of Δt improves the stability properties of the explicit Euler method. In this section we show how to extend the functions $\gamma_1(\Delta t)$ and $\gamma_2(\Delta t)$ to the multidimensional case obtaining semi-explicit NSFDs schemes, following Definition 2, with much better stability properties than the related SFDs method, for solving the problem (1.1). We use the word 'semi-explicit' because, as we will see, although the formulation of the methods suggests that they are linearly implicit schemes, it is possible to calculate offline the matrix to be inverted at each step, subsequently obtaining the advancing solution as a function of known quantities. Furthermore, in the next section we will prove that these extended functions also allow to obtain numerical methods that preserve the positivity of the exact solution of the model (1.1).

Let $\{t_n = t_0 + n\Delta t, n = 0, ..., N, t_N = T\}$ and $\{x_j = x_0 + j\Delta x, j = 0, ..., M+1, x_{M+1} = X\}$ be time and space discretizations of the domain. We then apply a spatial semi-discretization of the PDE system (1.1), using second order classical finite differences for the second order derivatives. From now on, $u_1^j(t)$, $u_2^j(t)$ and $w^j(t)$ represent approximations of $u_1(x_j, t)$, $u_2(x_j, t)$ and $w(x_j, t)$, respectively. For now, we set homogeneous Dirichlet boundary conditions. The resulting semi-discretized system can be written in the following form:

$$\begin{cases} \dfrac{dU_1}{dt} = \dfrac{1}{\Delta x^2} A_{Diff} U_1 + F_1, & F_1 = (w^j u_1^j (u_1^j + H u_2^j) - B_1 u_1^j - S u_1^j u_2^j)_{j=1}^M \in \mathbb{R}^M, \\ \dfrac{dU_2}{dt} = \dfrac{D}{\Delta x^2} A_{Diff} U_2 + F_2, & F_2 = (F w^j u_2^j (u_1^j + H u_2^j) - B_2 u_2^j)_{j=1}^M \in \mathbb{R}^M, \\ \dfrac{dW}{dt} = \dfrac{d}{\Delta x^2} A_{Diff} W + F_3, & F_3 = \big(A - w^j - w^j (u_1^j + u_2^j)(u_1^j + H u_2^j)\big)_{j=1}^M \in \mathbb{R}^M. \end{cases} \tag{4.4}$$

For simplicity, we have omitted the time dependence of u_1^j, u_2^j and w^j. The used notation is

$$U_1 = \big(u_1^j(t)\big)_{j=1}^M \in \mathbb{R}^M, \qquad U_2 = \big(u_2^j(t)\big)_{j=1}^M \in \mathbb{R}^M, \qquad W = \big(w^j(t)\big)_{j=1}^M \in \mathbb{R}^M,$$
$$\frac{dU_1}{dt} = \Big(\frac{du_1^j}{dt}\Big)_{j=1}^M \in \mathbb{R}^M, \qquad \frac{dU_2}{dt} = \Big(\frac{du_2^j}{dt}\Big)_{j=1}^M \in \mathbb{R}^M, \qquad \frac{dW}{dt} = \Big(\frac{dw^j}{dt}\Big)_{j=1}^M \in \mathbb{R}^M.$$

The matrix A_{Diff} obviously contains the spatial semi-discretization coefficients:

$$A_{Diff} = \begin{pmatrix} -2 & 1 & 0 & ... & 0 & 0 \\ 1 & -2 & 1 & 0 & ... & 0 \\ & & . & . & . & \\ 0 & 0 & ... & 0 & 1 & -2 \end{pmatrix} \in \mathbb{R}^{M,M}, \tag{4.5}$$

The semi-discretized system (4.4) can also be expressed in the following more compact form:

$$\frac{dY}{dt} = A_B Y + F,$$

$$Y = (U_1^T, U_2^T, W^T)^T \in \mathbb{R}^{3M}, \quad \frac{dY}{dt} = \Big(\frac{dU_1}{dt}^T, \frac{dU_2}{dt}^T, \frac{dW}{dt}^T\Big)^T \in \mathbb{R}^{3M}, \quad F = (F_1^T, F_2^T, F_3^T)^T \in \mathbb{R}^{3M}.$$

Here, the matrix A_B is a block diagonal matrix of the following type:

$$A_B = \frac{1}{\Delta x^2}\begin{pmatrix} A_{Diff} & 0 & 0 \\ 0 & DA_{Diff} & 0 \\ 0 & 0 & dA_{Diff} \end{pmatrix} \in \mathbb{R}^{3M,3M}. \tag{4.6}$$

Solving the obtained ODE system with explicit Euler method (2.2) leads to

$$Y_{n+1} = (\Delta t A_B + I)Y_n + \Delta t F_n, \quad n = 0, ..., N-1. \tag{4.7}$$

Here, I represents the Identity matrix of order $3M$, Y_n is an approximation of all the components of Y at $t = t_n$, and the same holds for F_n relative to F. Let us call Standard Euler (SE) the SFDs scheme (4.7) for the model (1.1).

Now, we prove that the SE method has very strong restrictions on the choice of Δt so that the numerical solution does not explode with increasing time. Therefore, it is not unconditionally stable.

Remark 2. *To analyze the stability properties of the methods discussed in this paper, we consider only the linear stiff part of the model* (1.1)*. This procedure is connected to what is usually done for the stability study of reaction-diffusion PDEs [32]. Here, the modified test equation $y'(t) = \lambda y(t) + \mu y(t)$ is considered, where λ is referred to the linear stiff diffusion part of the model and assumes significant importance, and μ to that of reaction and has little weight. Subsequently, widely used approaches are of IMplicit-EXplicit type, i.e. the stiff part of the model is solved by means of an implicit method, and the non-stiff part by means of an explicit one. In this section we derive methods stabilizing the stiff part of the model, then following a similar strategy.*

Proposition 2. *The standard scheme $Y_{n+1} = (\Delta t A_B + I)Y_n$ is stable if*

$$\Delta t < min\Big(\frac{\Delta x^2}{2}, \frac{\Delta x^2}{2D}, \frac{\Delta x^2}{2d}\Big). \tag{4.8}$$

Proof. We have to find the conditions guaranteeing that the spectral radius of the matrix $R = \Delta t A_B + I$ is less than one. The matrix R has three diagonal blocks, and each of them is constituted by a tridiagonal Toeplitz matrix [24] with equal elements on the two codiagonals and all zeros outside them and the main diagonal. We call (a_i, b_i), $i = 1, 2, 3$, the pairs '(diagonal element, codiagonal elements)' of the i-th block:

$$(a_1, b_1) = \Big(-2\frac{\Delta t}{\Delta x^2} + 1, \frac{\Delta t}{\Delta x^2}\Big), \quad (a_2, b_2) = \Big(-2D\frac{\Delta t}{\Delta x^2} + 1, \frac{D\Delta t}{\Delta x^2}\Big), \quad (a_3, b_3) = \Big(-2d\frac{\Delta t}{\Delta x^2} + 1, \frac{d\Delta t}{\Delta x^2}\Big).$$

The eigenvalues of R correspond to those of the tridiagonal matrices that form each block. For Toeplitz matrices of order M of this type, they are [33]

$$\lambda_k = a - 2bcos\Big(\frac{k\pi}{M+1}\Big), \quad k = 1, ..., M, \tag{4.9}$$

where a and b represent the diagonal and codiagonals elements, respectively.

In our case, imposing that $|\lambda_k| < 1$ for all the couples $(a, b) = (a_i, b_i)$, $i = 1, 2, 3$, is equivalent to require that $\lambda_k > -1$, as λ_k is always less than one. Since λ_k takes on a minimum value when the cosine approaches one, the final condition we must impose is $a - 2b > -1$. Request this condition for all three blocks, that is, for all pairs $(a, b) = (a_i, b_i)$, $i = 1, 2, 3$, leads exactly to the conditions (4.8). □

4.2. Construction of the nonstandard methods

Our goal, in this section, is to introduce NSFDs methods based on EF to follow the oscillating trend of the exact solution of the model (1.1), which are also able to make the SE method stability conditions (4.8) less restrictive.

Firstly, let us modify the standard discretization of the spatial second order derivative introduced in the semi-discrete system (4.4) using the EF, as shown in Section 3. Then, we replace the power Δx^2 with the function $\phi(\Delta x)$ (3.10). In this way, the matrix A_B (4.6) becomes

$$\tilde{A_B} = \frac{1}{\phi(\Delta x)} \begin{pmatrix} A_{Diff} & 0 & 0 \\ 0 & DA_{Diff} & 0 \\ 0 & 0 & dA_{Diff} \end{pmatrix} \in \mathbb{R}^{3M,3M}.$$

Therefore, the SE method (4.7) becomes a nonstandard scheme of the following form:

$$Y_{n+1} = (\Delta t \tilde{A_B} + I)Y_n + \Delta t F_n, \quad n = 0, ..., N-1. \tag{4.10}$$

Note that the stability conditions related to this scheme are very similar to those of the SE method (4.8). The only difference trivially lies in the presence of $\phi(\Delta x)$ instead of Δx^2. Remembering that, for the relation (3.11), $\phi(\Delta x)$ is very close to Δx^2, this does not lead to substantial changes.

Now, we extend the functions $\gamma_1(\Delta t)$ (4.1) and $\gamma_2(\Delta t)$ (4.2) to the multidimensional case, then replacing Δt in the SE version (4.10) with the new matrices thus obtained. In this way, we derive two NSFDs methods in accordance with Definition 2, proving that they are much more stable than the related SFDs scheme (4.7).

The extension of the function $\gamma_1(\Delta t)$ (4.1) we consider is the following:

$$\tilde{\varphi_1}(\Delta t) = \tilde{A_B}^{-1}(e^{\Delta t \tilde{A_B}} - I) \in \mathbb{R}^{3M,3M}. \tag{4.11}$$

Therefore, the SE version (4.10) becomes

$$Y_{n+1} = e^{\Delta t \tilde{A_B}} Y_n + \tilde{\varphi_1}(\Delta t) F_n, \quad n = 0, ..., N-1. \tag{4.12}$$

Let us call the scheme (4.12) Exponentially Fitted NonStandard Exponential (EFNSE) method. Note that this method corresponds to the classic exponential Euler using the matrix A_B, with the standard spatial second order derivative discretization, instead of $\tilde{A_B}$. Therefore, there is a close connection between NSFDs, TASE technique, and exponential methods. Note also that the matrix $\tilde{A_B}$ is a function of the spatial step-size Δx. Hence, the function $\tilde{\varphi_1}(\Delta t)$ also depends on Δx. However, since the next results hold for any choice of $\Delta x > 0$, we omit this dependency for simplicity of notation.

In order to demonstrate that the EFNSE method is an NSFDs scheme according to Definition 2, we have to prove that $\tilde{\varphi_1}(\Delta t)$ is positive semi-definite for each choice of $\Delta t > 0$, and that it approximates $I\Delta t$, for $\Delta t \to 0$. The last property is trivial from the Taylor series expansion of $\gamma_1(\Delta t)$ (4.3). We now prove the first property.

Theorem 3. *The matrix function $\tilde{\varphi_1}(\Delta t)$ (4.11) is positive definite.*

Proof. To carry out the proof, we demonstrate that $\tilde{\varphi_1}(\Delta t)$ is symmetric and has all positive eigenvalues [4].

To prove symmetry, we need $\tilde{A_B}^{-1}$ and $e^{\Delta t \tilde{A_B}} - I$ to be both symmetric and to commute. The matrix $\tilde{A_B}$ is real and symmetric, so the same is true for its inverse. Hence, it holds that

$$\tilde{A_B} = PD_BP^T, \text{ therefore } \tilde{A_B}^{-1} = PD_B^{-1}P^T,$$

where D_B and D_B^{-1} are diagonal matrices. For the properties of matrix exponentials, it holds also that

$$e^{\Delta t\tilde{A_B}} = Pe^{\Delta tD_B}P^T, \text{ therefore } e^{\Delta t\tilde{A_B}} - I = P(e^{\Delta tD_B} - I)P^T. \tag{4.13}$$

Here, $e^{\Delta tD_B}$ is a diagonal matrix having in place '(i,i)' the exponential of the element $\Delta tD_{B(i,i)}$. Therefore, the matrix $e^{\Delta tD_B} - I$ is also diagonal. We are in the real case. Hence, for the shown relation (4.13) and the made observations, the matrix $e^{\Delta t\tilde{A_B}} - I$ is symmetric. From the last two relations, it follows that $\tilde{A_B}^{-1}$ and $e^{\Delta t\tilde{A_B}} - I$ are simultaneously diagonalizable, as they have the same eigenvectors. Therefore, they commute [27] (Theorem 1.3.12).

Let us now prove that all the eigenvalues of $\tilde{\varphi_1}(\Delta t)$ are positive. Since $\tilde{A_B}^{-1}$ and $e^{\Delta t\tilde{A_B}} - I$ have the same eigenvectors, an eigenvalue of $\tilde{\varphi_1}(\Delta t)$ is given by the product of an eigenvalue of $\tilde{A_B}^{-1}$ and one of $e^{\Delta t\tilde{A_B}} - I$. The eigenvalues of $\tilde{A_B}$ are the ones that form each matrix block. They are again given by the formula (4.9). In this case the couples $(a,b) = (a_i, b_i), i = 1,2,3$, are

$$(a_1,b_1) = \Big(-\frac{2}{\phi(\Delta x)}, \frac{1}{\phi(\Delta x)}\Big), (a_2,b_2) = \Big(-\frac{2D}{\phi(\Delta x)}, \frac{D}{\phi(\Delta x)}\Big), (a_3,b_3) = \Big(-\frac{2d}{\phi(\Delta x)}, \frac{d}{\phi(\Delta x)}\Big). \tag{4.14}$$

Let us call μ_k, $k = 1,...,3M$, all the eigenvalues of $\tilde{A_B}$. The eigenvalues of $\tilde{A_B}^{-1}$ are $1/\mu_k$, $k = 1,...,3M$. Note that $\mu_k < 0$, $\forall k = 1,...,3M$. These eigenvalues also correspond to the diagonal elements of D_B. Therefore, the diagonal elements of $e^{\Delta tD_B} - I$ are $e^{\Delta t\mu_k} - 1$, $k = 1,...,3M$. The latter exactly correspond to the eigenvalues of $e^{\Delta t\tilde{A_B}} - I$. Since the exponential of a negative number is always between zero and one, the eigenvalues of $e^{\Delta t\tilde{A_B}} - I$ are all negative. In conclusion, the eigenvalues of $\tilde{\varphi_1}(\Delta t)$ are all positive. □

Let us now prove that the EFNSE method has much better stability than SE method.

Theorem 4. *The NSFDs scheme $Y_{n+1} = e^{\Delta t\tilde{A_B}}Y_n$ is unconditionally stable.*

Proof. We have to prove that the spectral radius of $e^{\Delta t\tilde{A_B}}$ is always less than one. The eigenvalues of $\Delta t\tilde{A_B}$ are again given by the formula (4.9). Looking at the eigenvalues of $\tilde{A_B}$ (4.14), the couples $(a,b) = (a_i, b_i), i = 1,2,3$, now are

$$(a_1,b_1) = \Big(-2\frac{\Delta t}{\phi(\Delta x)}, \frac{\Delta t}{\phi(\Delta x)}\Big), \quad (a_2,b_2) = \Big(-2D\frac{\Delta t}{\phi(\Delta x)}, \frac{D\Delta t}{\phi(\Delta x)}\Big), \quad (a_3,b_3) = \Big(-2d\frac{\Delta t}{\phi(\Delta x)}, \frac{d\Delta t}{\phi(\Delta x)}\Big).$$

Note that all the eigenvalues of $\Delta t\tilde{A_B}$ are therefore negative. Let us call them $\mu_k, k = 1,...,3M$. For the considerations made in the previous theorem, the eigenvalues of $e^{\Delta t\tilde{A_B}}$ are $e^{\mu_k}, k = 1,...,3M$. Therefore, no eigenvalue of $e^{\Delta t\tilde{A_B}}$ has modulus equal to one or greater than one. □

The considerations made so far allow to conclude that EFNSE (4.12) is a semi-explicit NSFDs method with much better stability properties than the relative SFDs scheme. However, EFNSE is quite expensive as it requires the computation of a big dimension matrix exponential and a matrix inverse. For this reason, we now propose an alternative nonstandard method that does not involve the calculation of a matrix exponential.

For this purpose, let us substitute Δt in the SE version (4.10) with an extension to the multidimensional case of the function $\gamma_2(\Delta t)$ (4.2). The function we consider in the non-scalar case is

$$\tilde{\varphi_2}(\Delta t) = \Delta t(I - \Delta t\tilde{A_B})^{-1} \in \mathbb{R}^{3M,3M}. \tag{4.15}$$

Therefore, the SE version (4.10) becomes

$$Y_{n+1} = (I - \Delta t \tilde{A_B})^{-1} Y_n + \tilde{\varphi_2}(\Delta t) F_n, \quad n = 0, ..., N-1. \tag{4.16}$$

Let us call it Exponentially Fitted NonStandard Rational (EFNSR) method.

The NSR method is explicit by structure, even if we were inspired by implicit Euler. Indeed, the matrix $(I - \Delta t \tilde{A_B})^{-1}$ is constant, and therefore of course also $\tilde{\varphi_2}(\Delta t)$ is constant. Hence, once the matrix $(I - \Delta t \tilde{A_B})^{-1}$ has been computed before launching the method, it does not need to be updated at each step. In order to demonstrate that EFNSR is an NSFDs method according to Definition 2, we have only to prove that $\tilde{\varphi_2}(\Delta t)$ is positive semi-definite for each choice of $\Delta t > 0$. In fact, it trivially approximates $I\Delta t$, for $\Delta t \to 0$. For the same reasons explained above, we omit the Δx dependency of $\tilde{\varphi_2}(\Delta t)$.

Theorem 5. *The matrix function $\tilde{\varphi_2}(\Delta t)$ (4.15) is positive definite.*

Proof. To make the proof, we demonstrate that $\Delta t(I - \Delta t \tilde{A_B})^{-1}$ is symmetric and has positive eigenvalues. Observe that the symmetry is trivial from the fact that $\tilde{A_B}$ is symmetric. Furthermore, in Theorem 3 we proved that all the eigenvalues of $\tilde{A_B}$ are negative. Therefore, all the eigenvalues of $I - \Delta t \tilde{A_B}$ are positive, and the same is trivially true for the matrix $\Delta t(I - \Delta t \tilde{A_B})^{-1}$. □

To conclude, we demonstrate that the EFNSR method (4.16) has much better stability properties than the related SFDs one (4.7).

Theorem 6. *The NSFDs scheme $Y_{n+1} = (I - \Delta t \tilde{A_B})^{-1} Y_n$ is unconditionally stable.*

Proof. We have to prove that the spectral radius of $(I - \Delta t \tilde{A_B})^{-1}$ is always less than one. The eigenvalues of $I - \Delta t \tilde{A_B}$ are given by the formula (4.9). Looking at the eigenvalues of $\tilde{A_B}$ (4.14), the couples $(a, b) = (a_i, b_i), i = 1, 2, 3$, now are

$$(a_1, b_1) = \Big(1+2\frac{\Delta t}{\phi(\Delta x)}, \frac{\Delta t}{\phi(\Delta x)}\Big), (a_2, b_2) = \Big(1+2D\frac{\Delta t}{\phi(\Delta x)}, \frac{D\Delta t}{\phi(\Delta x)}\Big), (a_3, b_3) = \Big(1+2d\frac{\Delta t}{\phi(\Delta x)}, \frac{d\Delta t}{\phi(\Delta x)}\Big).$$

Note that all the eigenvalues of $I - \Delta t \tilde{A_B}$ are greater than one. Therefore, the eigenvalues of $(I - \Delta t \tilde{A_B})^{-1}$ are less than one. □

In this section, we have shown that modifications of explicit Euler scheme for our model, applying an extension of the NSFDs technique, lead to much more stable numerical methods. It is important to underline that the EFNSE (4.12) and EFNSR (4.16) methods preserve their explicit structure. The only additional functions evaluations with respect to the SE method concern the computation of the exponential and the inverse of a matrix for the first, and of the inverse of a matrix for the latter, before launching the method.

5. Positivity preservation by nonstandard schemes

In this section, we show how it is possible to further modify the EFNSE (4.12) and EFNSR (4.16) methods, this time using the second rule of NSFDs, to impose that the computed numerical solution is always non-negative. In fact, as mentioned in the Introduction, the considered model (1.1) is positive. Therefore, we want that the used numerical methods preserve this characteristic.

Let us give the definitions of positivity of a PDE system and of a numerical method.

Definition 3. *[35] Consider the PDE model* (1.1)*, defining* $y(x,t) := \big(u_1(x,t), u_2(x,t), w(x,t)\big)$*. Therefore, the domain of the function* y *is* Ω*, and the codomain is* $\mathbb{R}^3$*. The PDE system is positive if it holds that*

$$y(x,t_0) \geq 0, \quad \forall x \in [x_0, X] \quad \Longrightarrow \quad y(x,t) \geq 0, \quad \forall (x,t) \in \Omega.$$

Requiring that the function y *is non-negative means requiring that all its components are non-negative. Obviously, this definition can be extended to any system of PDEs.*

Definition 4. *[35] Consider a generic numerical method for solving the PDE system* (1.1) *along the discrete rectangular grid* $\{x_j = x_0 + j\Delta x, j = 0, ..., M+1, x_{M+1} = X\} \times \{t_n = t_0 + n\Delta t, n = 0, ..., N, t_N = T\}$*. The method is positive if it holds that*

$$y(x_j, t_0) \geq 0, \quad \forall j = 0, ..., M+1 \quad \Longrightarrow \quad y_n^j \approx y(x_j, t_n) \geq 0, \quad \forall j = 0, ..., M+1, \quad \forall n = 1, ..., N.$$

Look at the SE scheme (4.7) for the model (1.1). Note that, in order for it to produce non-negative solutions, the right part must be non-negative for every value of $n \geq 0$. Suppose that Y_0 has all non-negative components. Therefore, sufficient conditions for the positivity of the SFDs method are

$$\Delta t A_B + I \geq 0, \qquad F_n \geq 0, \quad \forall n = 0, ..., N-1.$$

Now and onward, requiring that matrices or vectors are non-negative corresponds to require that all their entries or components are non-negative, respectively. Note that $\Delta t A_B + I \geq 0$ if the SE stability conditions (4.8) are met. Hence, we have very stringent restrictions on the choice of the step-sizes for the SE method (4.7) to be positive.

Let us consider the EFNSE method (4.12). In this case, sufficient conditions for its positivity are

$$e^{\Delta t \tilde{A_B}} \geq 0, \qquad \tilde{\varphi_1}(\Delta t) \geq 0, \qquad F_n \geq 0, \quad \forall n = 0, ..., N-1.$$

Instead, regarding the EFNSR method (4.16), sufficient conditions for its positivity are

$$(I - \Delta t \tilde{A_B})^{-1} \geq 0, \qquad \tilde{\varphi_2}(\Delta t) \geq 0, \qquad F_n \geq 0, \quad \forall n = 0, ..., N-1.$$

Note that the non-negativity of F_n is not taken for granted. However, we can obtain it by modifying the nonstandard numerical schemes derived in the previous section using the second rule of the NSFDs.

Consider the columns vectors F_1, F_2 and F_3 previously defined (4.4). Let us split each of them into two separate ones as follows, setting $\mathbb{1}_M = (1, ..., 1) \in \mathbb{R}^M$:

$$\begin{aligned}
F_1^L &= \big(w^j u_1^j (u_1^j + H u_2^j)\big)_{j=1}^M \in \mathbb{R}^M, \qquad F_1^{NL} = (B_1 + S u_2^j)_{j=1}^M \in \mathbb{R}^M, \\
F_2^L &= \big(F w^j u_2^j (u_1^j + H u_2^j)\big)_{j=1}^M \in \mathbb{R}^M, \qquad F_2^{NL} = \mathbb{1}_M B_2 \in \mathbb{R}^M, \\
F_3^L &= \mathbb{1}_M A \in \mathbb{R}^M, \qquad F_3^{NL} = \big(1 + (u_1^j + u_2^j)(u_1^j + H u_2^j)\big)_{j=1}^M \in \mathbb{R}^M.
\end{aligned}$$

For simplicity, we have again omitted the time dependence of u_1^j, u_2^j and w^j.

Now, we compact the column vectors just defined in the following way:

$$F^L = \big((F_1^L)^T, (F_2^L)^T, (F_3^L)^T\big)^T \in \mathbb{R}^{3M}, \qquad F^{NL} = \big((F_1^{NL})^T, (F_2^{NL})^T, (F_3^{NL})^T\big)^T \in \mathbb{R}^{3M}.$$

Observe that multiplying component by component $(u_1^j)_{j=1}^M$, $(u_2^j)_{j=1}^M$ and $(w^j)_{j=1}^M$, for F_1^{NL}, F_2^{NL} and F_3^{NL}, respectively, then adding F^L with the resulting F^{NL}, we get just the vector F. Note also that in the SFDs and NSFDs methods derived so far, the vector F is evaluated exclusively at t_n to determine the numerical solution at t_{n+1}. Alternatively, we now introduce non-local representations, evaluating some non-linear terms at t_{n+1}, as follows:

$$Y_{n+1} *.(\mathbb{1}_{3M} + \tilde{\varphi_1}(\Delta t)F_n^{NL}) = e^{\Delta t \tilde{A_B}} Y_n + \tilde{\varphi_1}(\Delta t)F_n^L, \quad n = 0, ..., N-1,$$

$$Y_{n+1} *.(\mathbb{1}_{3M} + \tilde{\varphi_2}(\Delta t)F_n^{NL}) = (I - \Delta t \tilde{A_B})^{-1} Y_n + \tilde{\varphi_2}(\Delta t)F_n^L, \quad n = 0, ..., N-1.$$

Here, the symbol '$*.$' indicates the component by component product of the involved vectors.

The derived formulas are NSFDs methods for the model (1.1). They have been obtained by further modifying the EFNSE (4.12) and EFNSR (4.16) methods, respectively.

The new schemes are still explicit by structure. In fact, they can be rewritten as

$$Y_{n+1} = (e^{\Delta t \tilde{A_B}} Y_n + \tilde{\varphi_1}(\Delta t)F_n^L)/.(\mathbb{1}_{3M} + \tilde{\varphi_1}(\Delta t)F_n^{NL}), \quad n = 0, ..., N-1, \tag{5.1}$$

$$Y_{n+1} = \big((I - \Delta t \tilde{A_B})^{-1} Y_n + \tilde{\varphi_2}(\Delta t)F_n^L\big)/.(\mathbb{1}_{3M} + \tilde{\varphi_2}(\Delta t)F_n^{NL}), \quad n = 0, ..., N-1, \tag{5.2}$$

where the symbol '$/.$' indicates the component by component ratio of the involved vectors. Let us call these methods EFNSE Positive (EFNSEP) (5.1) and EFNSR Positive (EFNSRP) (5.2), respectively. In fact, we now prove their positivity with no restrictions on the choice of discretization steps.

Theorem 7. *The EFNSEP* (5.1) *and EFNSRP* (5.2) *methods are unconditionally positive.*

Proof. Proceeding by induction, assuming $Y_n \geq 0$, and then F_n^L, $F_n^{NL} \geq 0$ since the model parameters are all positive, to get $Y_{n+1} \geq 0$ it is sufficient to prove that $e^{\Delta t \tilde{A_B}}$ and $(I - \Delta t \tilde{A_B})^{-1}$ have all non-negative entries. Indeed, the functions $\tilde{\varphi_1}(\Delta t)$ and $\tilde{\varphi_2}(\Delta t)$ are approximation of $I\Delta t$. Therefore, we can suppose their non-negativity.

Observe that the matrix $\Delta t \tilde{A_B}$ is essentially non-negative, as its off diagonal entries are all non-negative. Therefore $e^{\Delta t \tilde{A_B}} \geq 0$ [25] (Theorem 10.29).

Note also that $I - \Delta t \tilde{A_B}$ is an M-matrix [37]. In fact, it has all non-negative real eigenvalues, as shown in Theorem 6, and its off diagonal entries are all non-positive [3]. Since the inverse of an M-matrix has all non-negative entries [37], then $(I - \Delta t \tilde{A_B})^{-1} \geq 0$. Note that this also proves the non-negativity of $\tilde{\varphi_2}(\Delta t)$ for each choice of $\Delta t > 0$. □

Note that applying the second NSFDs rule to preserve positivity adds implicitness to the non-linear terms of F. Usually, by doing this, the stability of the method further improves. This will be confirmed in numerical tests. Note also that if we had not modified the standard method using the proposed multidimensional functions, it would not have been possible to preserve positivity without stringent conditions on the step-size in time.

To conclude, let us prove the consistency of all the derived NSFDs methods. In fact, they solve the PDE system (1.1) with accuracy order equal to one in time and two in space.

Theorem 8. *The Local Truncation Error (LTE) of the NSFDs methods derived in this paper for the numerical solution of the PDE system* (1.1) *is*

$$LTE = O(\Delta t) + O(\Delta x^2).$$

Proof. Let $\varphi(\Delta t)$ be a scalar function satisfying $\varphi(\Delta t) = \Delta t + O(\Delta t^2)$, for $\Delta t \to 0$. Moreover, let $\phi(\Delta x)$ be a scalar function satisfying $\phi(\Delta x) = \Delta x^2 + O(\Delta x^4)$, for $\Delta x \to 0$. We use the notation $u_{1n}^j \approx u_1(x_j, t_n)$, $u_{2n}^j \approx u_2(x_j, t_n)$, $w_n^j \approx w(x_j, t_n)$. The EFNSE, EFNSR, EFNSEP and EFNSRP methods can be expressed as

$$\frac{u_{n+1}^j - u_n^j}{\varphi(\Delta t)} = d_u \frac{u_n^{j+1} - 2u_n^j + u_n^{j-1}}{\phi(\Delta x)} + f_u(y_n^j, u_{n+1}^j),$$

where u corresponds to u_1, u_2, or w, and $y = (u_1, u_2, w)$. Moreover, the constant d_u and the reaction function f_u change according to the model component and method considered.

Note that $LTE = O(\Delta t)$ in the discretization of the time derivative, as it holds that

$$u(x_j, t_{n+1}) - u(x_j, t_n) = \varphi(\Delta t) \frac{\partial u(x_j, t_n)}{\partial t} + O(\Delta t^2).$$

This follows from the hypothesis $\varphi(\Delta t) = \Delta t + O(\Delta t^2)$ and from the known relation

$$u(x_j, t_{n+1}) - u(x_j, t_n) = \Delta t \frac{\partial u(x_j, t_n)}{\partial t} + O(\Delta t^2).$$

Furthermore, $LTE = O(\Delta x^2)$ in the discretization of the spatial derivative, as it holds that

$$u(x_{j+1}, t_n) - 2u(x_j, t_n) + u(x_{j-1}, t_n) = \phi(\Delta x) \frac{\partial^2 u(x_j, t_n)}{\partial x^2} + O(\Delta x^4).$$

This follows from the hypothesis $\phi(\Delta x) = \Delta x^2 + O(\Delta x^4)$ and from the known relation

$$u(x_{j+1}, t_n) - 2u(x_j, t_n) + u(x_{j-1}, t_n) = \Delta x^2 \frac{\partial^2 u(x_j, t_n)}{\partial x^2} + O(\Delta x^4).$$

Finally, $LTE = O(\Delta t)$ in the discretization of the reaction term, as it holds that

$$u(x_j, t_{n+1}) = u(x_j, t_n) + O(\Delta t).$$

Actually, $LTE = 0$ for the reaction term of the EFNSE and EFNSR methods, as in that case f_u is only a function of y_n^j. From the considerations made, the theorem follows. □

6. Numerical results

In order to verify all the theoretical considerations made so far regarding the better stability of the EFNSE and EFNSR methods with respect to the SFDs one (4.7), the positivity of the EFNSEP and EFNSRP schemes and the advantages of the EF, in this section we apply to the model (1.1) all the NSFDs methods derived in this paper. Furthermore, to compare the methods derived in this work with methods existing in the literature, we also consider explicit Runge-Kutta Chebyshev (RKC) methods [45]. They were in fact introduced to solve stiff systems of ODEs that originate from parabolic PDEs. Since we have derived methods of temporal order equal to one, to have a fair comparison we choose the RKC method of order one derived in the paper [45], which has even better stability than RKC schemes of higher order.

We divide this section into two subsections. In the first one, we evaluate the performance of the new methods only over time by fixing Δx and varying Δt. In the second one, we evaluate the behavior of the methods also in space.

The PDE system is solved using periodic boundary conditions. Therefore, the matrix A_{Diff} (4.5) slightly changes increasing by one its dimension and putting one in place of zero in the last position of the first row and first column, as follows:

$$A_{Diff} = \begin{pmatrix} -2 & 1 & 0 & ... & 0 & 1 \\ 1 & -2 & 1 & 0 & ... & 0 \\ & . & . & . & & \\ 1 & 0 & ... & 0 & 1 & -2 \end{pmatrix} \in \mathbb{R}^{M+1,M+1}.$$

In this case it is necessary to add the initial component (i.e. the one corresponding to $j = 0$) to the vectors defined in the semi-discretized system (4.4) and to those declared immediately after. Obviously, A_B, $\tilde{A_B}$, $\tilde{\varphi_1}(\Delta t)$ and $\tilde{\varphi_2}(\Delta t)$ are then modified accordingly.

Remark 3. *The results demonstrated for homogeneous boundary conditions in Section 4 and in Section 5 continue to be valid also for periodic boundary conditions. To prove this, just observe that the new matrix $\tilde{A}_B$ continues to be real and symmetric. Furthermore, its eigenvalues are non-positive for the first Gerschgorin Theorem. The only difference from the homogeneous case lies in its singularity. For this reason, in practice ad hoc algorithms are used for the calculation of functions such as $\tilde{\varphi_1}(\Delta t)$ which avoid the direct computation of $\tilde{A}_B^{-1}$ (see, e.g., [26, 36]).*

As mentioned above, a choice for performing numerical tests may lie in the a-priori computation of the functions $\tilde{\varphi_1}(\Delta t)$ and $\tilde{\varphi_2}(\Delta t)$. Alternatively, regarding the schemes involving the exponential function $\tilde{\varphi_1}(\Delta t)$, there are several iterative methods that efficiently and directly compute the function-vector product appearing in the method (see, e.g., [36]). Regarding instead the methods involving $\tilde{\varphi_2}(\Delta t)$, one can proceed by initially determining a single LU-decomposition of the matrix to be inverted, subsequently solving a linear system for each step. In this paper, we a-priori compute the function $\tilde{\varphi_1}(\Delta t)$ using the Matlab code 'phim', which is part of the package 'exp4' [26]. This code was purposely built to numerically evaluate the function $z^{-1}(e^z - 1)$, where z represents a generic matrix. Furthermore, we proceed by solving one linear system per step, by a-priori computing the LU-decomposition of $\tilde{\varphi_2}(\Delta t)$ given by the Matlab *lu* function, for the EFNSR and EFNSRP methods.

The value $\omega = \pi/10$ corresponds to the spatial asymptotic oscillation frequency of the exact solution and has been estimated by means of a reference solution determined as explained later. The model parameters values are

$$A = 1.5; \quad B_1 = 0.45; \quad B_2 = 0.3611; \quad D, G, H = 0.802; \quad S = 0.0002; \quad d = 500.$$

6.1. First part

In this subsection, we solve the PDE system (1.1) over the rectangular grid $[-50, 50] \times [0, 600]$, setting the initial values of the solution randomly in the interval $[1.4, 2.1]$ for u_1 and u_2, and in the interval $[0.14, 0.21]$ for w. In particular, we use the Matlab *rand* function to generate the random values of these components, setting the state at 10. Proceeding in this way makes the results easily replicable, and in any case similar to those reproduced in the paper [21], in which random perturbations of the equilibrium states are used as initial conditions. Furthermore, fixed the number of spatial grid points, we can always use the same initial conditions, being able to compare the errors of the various

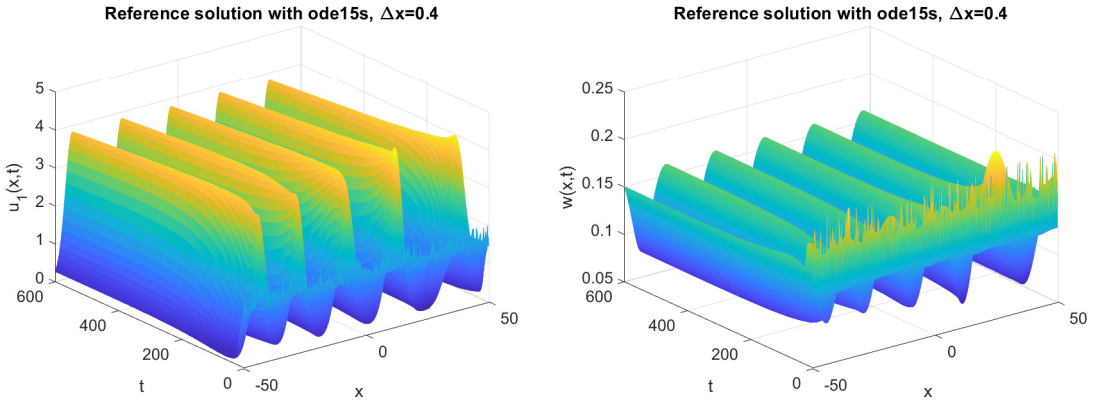

Figure 1: Components u_1 and w of the reference solution, calculated using the *ode15s* Matlab function, $\Delta x = 0.4$.

methods used. The reference solution is computed by applying the Matlab *ode*15*s* function to the semi-discretized problem (4.4), replacing Δx^2 with $\phi(\Delta x)$ (3.10), requiring maximum accuracy, i.e. setting the options arguments 'RelTol' and 'AbsTol' equal to the machine precision. We make this substitution because in this subsection we evaluate the trend of the methods only over time, 'neglecting' the spatial error. The relative errors are determined at the last time grid point $T = 600$ using norm two. In addition, we estimate the order in time of the methods with the formula $\big(cd(\Delta t) - cd(2\Delta t)\big)/log_{10}2$. Here, $cd(\Delta t)$ is an estimate of the number of correct digits obtained with step-size Δt, derived as $cd(\Delta t) = -log_{10}\big(error(\Delta t)\big)$.

We report in the following graphs and tables the results setting $M = 250$, so $\Delta x = 0.4$, also in the computation of the reference solution. Figures 1 and 2 show all the components of the exact solution. In Table 1 we report the relative errors obtained by applying the SE, EFNSE and EFNSR methods. In Figure 3 on the left we report a comparison between the EFNSE, EFNSR, and RKC methods, also from a CPU time point of view, including that for setting the data and coefficients (therefore also for the computation of the matrix exponential for EFNSE, and for the LU-factorization for EFNSR). Since we calculate the reference solution using $\phi(\Delta x)$ instead of Δx^2 in the semi-discretized system, we do the same with the SE method, for which we consider the version (4.10), and with the RKC method. Note that in this case $\phi(\Delta x) \approx 0.1598$ and $\Delta x^2 = 0.16$. Therefore, the stability conditions of the version (4.10) are substantially the same as those of the classic SE method (4.8), as already observed in the paper. They lead to $\Delta t < 1.598 \times 10^{-4}$. On the other hand, the EFNSE and EFNSR methods are able to provide good results for much larger Δt values, resulting therefore decidedly cheap and advantageous. Asymptotically, from Table 1, the EFNSE method seems more accurate than EFNSR. Regarding the RKC method, to have a stable solution for the same steps values used in Table 1, we have chosen $s = 20$, where s is the number of stages. In fact, the RKC stability condition is $\Delta t\sigma \leq \beta(s)$ [45], where σ is the spectral radius of the diffusion matrix and $\beta(s) \approx 1.93s^2$. From the left plot of Figure 3, note that the RKC method has the same behavior as the EFNSR method. On the other hand, the EFNSE method is slower than EFNSR and RKC, because the computation of the matrix exponential and the resulting matrix-vector product, where the matrix is dense, take longer. Observe that the EFNSR method is still more convincing than the RKC in computing a qualitatively good solution in a short time.

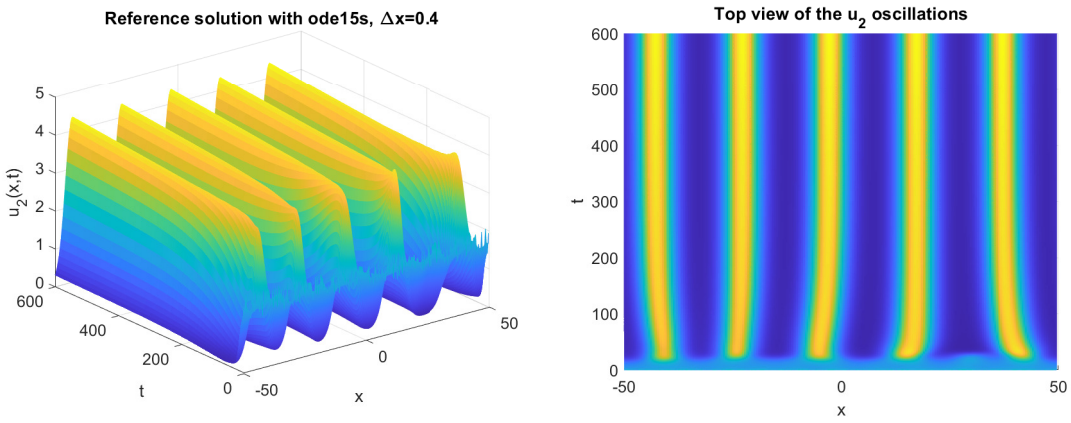

Figure 2: Component u_2 of the reference solution, calculated using the *ode15s* Matlab function, $\Delta x = 0.4$, and top view of its spatial oscillations.

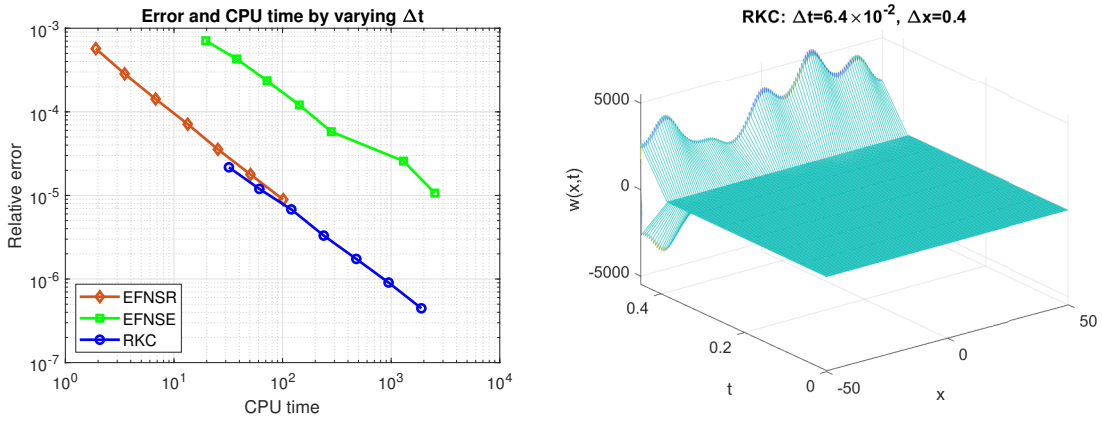

Figure 3: Efficiency plot with errors and CPU time for comparison between the EFNSE, EFNSR and RKC methods on the left, and numerical solution by the RKC method, setting $\Delta t = 0.065$, $\Delta x = 0.4$, on the right.

Table 1: Relative error and estimated order of SE, EFNSE and EFNSR methods, setting $M = 250$ and varying the number of intervals N into which we divide the time grid.

N	SE error	order	EFNSE error	order	EFNSR error	order
2^{14}	-	-	7.0910e-04	-	5.7045e-04	-
2^{15}	-	-	4.2935e-04	0.7238	2.8450e-04	1.0037
2^{16}	-	-	2.3513e-04	0.8687	1.4227e-04	0.9998
2^{17}	-	-	1.2078e-04	0.9611	7.1167e-05	0.9994
2^{18}	-	-	5.7860e-05	1.0617	3.5597e-05	0.9995
2^{19}	-	-	2.5758e-05	1.1675	1.7803e-05	0.9996
2^{20}	-	-	1.0663e-05	1.2724	8.9025e-06	0.9998
2^{21}	-	-	4.1754e-06	1.3526	4.4516e-06	0.9999
2^{22}	1.6906e-07	-	1.6648e-06	1.3266	2.2259e-06	0.9999
2^{23}	8.4564e-08	0.9994	7.1447e-07	1.2204	1.1130e-06	0.9999

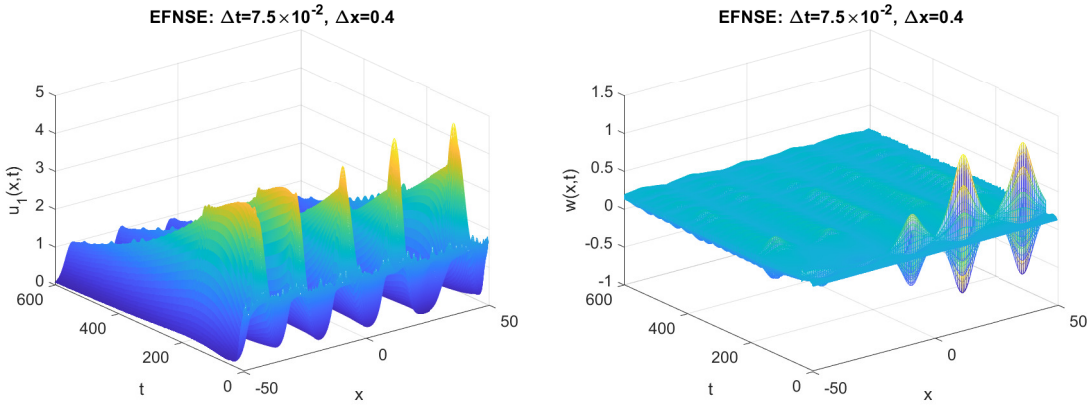

Figure 4: Numerical solution by the EFNSE method, setting $\Delta t = 0.075$, $\Delta x = 0.4$.

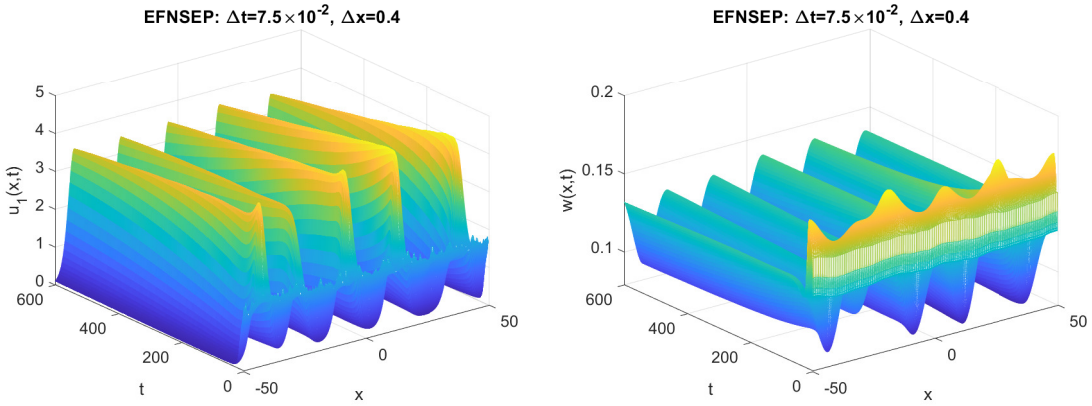

Figure 5: Numerical solution by the EFNSEP method, setting $\Delta t = 0.075$, $\Delta x = 0.4$.

Now, let us discuss the utility of positivity preserving schemes, whose errors are reported in Table 2. These schemes constitute a further modification of the EFNSE and EFNSR methods made for stability reasons. The positive methods are able to better preserve the qualitative trend of the exact solution even for very high values of Δt. From Figure 4, note that for $\Delta t = 0.075$ the EFNSE method produces a solution that is totally inconsistent with the exact one. In fact, it also yields negative values. For an even smaller step value, also the RKC method produces a solution which becomes negative and which is not stable, as shown in Figure 3 on the right. The EFNSEP method, on the other hand, produces a solution that not only remains always positive, as demonstrated also analytically, but reproduces the trend of the exact one qualitatively well. We can see it in Figure 5. Therefore, the positivity preserving methods have even better stability than the other NSFDs schemes derived in the paper. This is very important, as for predictive models the main interest lies in the knowledge of the long-term trend of the solution, without requiring high accuracy. The methods that preserve positivity are the cheapest of those derived in the paper to do this.

Finally, we show that the constructed NSFDs methods are able to preserve the metastability of

Table 2: Relative error and estimated order of EFNSEP and EFNSRP methods, setting $M = 250$.

N	EFNSEP error	order	EFNSRP error	order
2^{17}	4.0642e-02	-	6.3528e-02	-
2^{18}	2.2413e-02	0.8586	3.8715e-02	0.7145
2^{19}	1.1791e-02	0.9266	2.1746e-02	0.8321
2^{20}	6.0504e-03	0.9626	1.1592e-02	0.9076
2^{21}	3.0650e-03	0.9811	5.9958e-03	0.9511
2^{22}	1.5426e-03	0.9905	3.0507e-03	0.9748

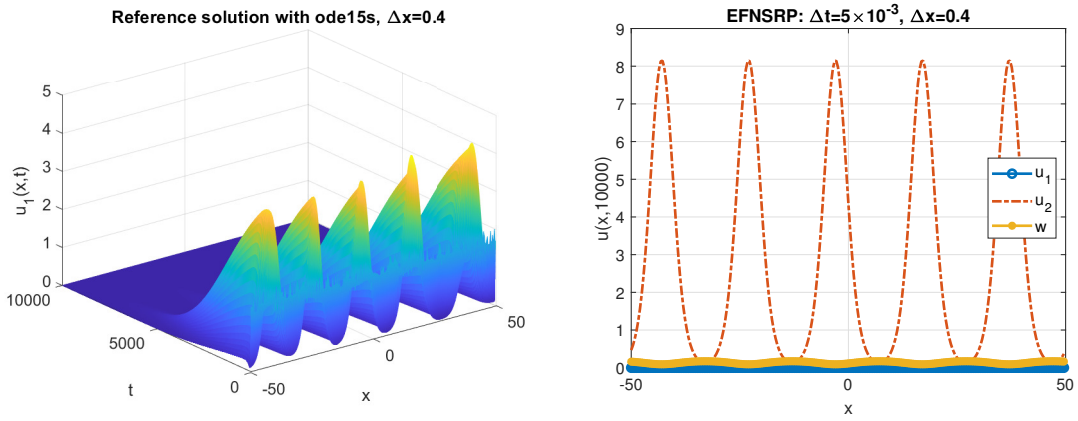

Figure 6: Component u_1 of the reference solution and numerical solution computed by the EFNSRP method at $t = 10000$.

the PDE system (1.1). In fact, in the Introduction we mentioned that after a considerable time one of the two plants dies. Figure 6 on the left shows that this happens for u_1. Figure 6 on the right shows the three components of the solution at $t = 10000$ computed using the EFNSRP method. Note that this NSFDs method is adept at preserving metastability even though it was not built for this purpose, also for a larger time step-size than those used in Table 2. We have verified that all the other NSFDs methods proposed in this paper preserve metastability for large time steps.

6.2. Second part

In this subsection, we evaluate the behavior of the considered methods also in space, setting the same grid as before. To do this, we need to change the initial conditions used in the previous subsection. In fact, using the Matlab *rand* function again, variations in the spatial step-size Δx would correspond to different initial conditions each time. Given the observed behavior of the exact solution, we initially set $u_1(x,0), u_2(x,0) = cos(\pi x/10) + 1$, and $w(x,0) = (1/10)cos(\pi x/10) + 1/10$. At the end of this subsection, we also show that using different functions as initial conditions, the asymptotic frequency of the reference solution in space and the errors remain the same. Regarding the exponentially fitted methods, we now consider a classical second order centred spatial semi-discretization for the function w, as it produces oscillations with much lower amplitude compared to u_1 and u_2. The reference solution is obtained by applying the Matlab *ode*15*s* function requiring maximum accuracy to the semi-discrete system (4.4), this time setting $\Delta x = 0.025$. It takes about 10^4 seconds for the mentioned computation.

Table 3: Global relative error of the EFNSR, EFNSRP, RKC and SE methods.

Δx	Δt	EFNSR	EFNSRP	RKC	Δx	Δt	SE
2	0.0625	2.6443e-02	2.4167e-01	3.8976e-02	2	0.0025	3.8938e-02
$2/2$	$0.0625/2^2$	6.5252e-03	1.1942e-01	9.5457e-03	$2/2$	$0.0025/2^2$	9.5380e-03
$2/2^2$	$0.0625/2^4$	1.5881e-03	5.7509e-02	2.3282e-03	$2/2^2$	$0.0025/2^4$	2.3264e-03
$2/2^3$	$0.0625/2^6$	3.9040e-04	1.8848e-02	5.7449e-04	$2/2^3$	$0.0025/2^6$	5.7403e-04

Table 4: CPU times in seconds of the EFNSR, EFNSRP, RKC and SE methods related to the results of Table 3.

Δx	Δt	EFNSR	EFNSRP	RKC	Δx	Δt	SE
2	0.0625	1.1875e+00	1.4844e+00	5.3125e+00	2	0.0025	1.9828e+01
$2/2$	$0.0625/2^2$	3.7500e+00	5.4688e+00	1.9234e+01	$2/2$	$0.0025/2^2$	7.9188e+01
$2/2^2$	$0.0625/2^4$	1.5109e+01	4.0859e+01	7.7734e+01	$2/2^2$	$0.0025/2^4$	3.2770e+02
$2/2^3$	$0.0625/2^6$	7.1094e+01	1.2790e+03	3.2786e+02	$2/2^3$	$0.0025/2^6$	1.3579e+03

The trend of the exact solution is the same observed in the previous case, as shown in Figure 7 on the left, in which the component u_1 is reported.

We report in Table 3 on the left the global relative errors at the endpoint $T = 600$ obtained with respect to the reference solution, applying the EFNSR, EFNSRP and RKC methods. The latter is applied to the semi-discretized system (4.4), setting $s = 5$ for stability reasons. These errors are obtained by firstly setting $\Delta x = 2$ and $\Delta t = 0.0625$, then always halving Δx and dividing by four Δt. Note that the errors get four times smaller each time, which allows to conclude that the methods actually have order two in space. This is confirmed in Figure 7, on the right, where the error trend of the considered NSFDs methods is shown, by varying Δx, fixing $\Delta t = 0.0625/2^{10}$. In this subsection we have not considered the EFNSE and EFNSEP methods as they produce very similar results to the EFNSR and EFNSRP methods, respectively.

In order to be able to make a comparison even between the NSFDs schemes and the SE method (4.7), we need to set much smaller steps over time, in accordance with the SE stability conditions (4.8). Setting the same starting spatial step-size of Table 3, we must use $\Delta t < 4 \times 10^{-3}$ in order not to have an explosion of the solution. Therefore, using $\Delta t = 0.0025$ as the initial time step, and then carrying out the same operations as before, we obtain the results reported in the right part of Table 3. In Table 4, we report the CPU times employed by all the methods used to obtain the results of Table 3. To better visualize the results of Tables 3 and 4, we also realize a related efficiency plot in Figure 8 on the right. Observe that EFNSR is cheaper and more accurate than the other methods, thanks to its good stability properties and to the used exponentially fitted discretization for the second order derivative. We also note that the EFNRP method is the least efficient. In fact, as seen before, it is advantageous when a qualitatively good solution is required using very large steps over time.

To conclude this subsection, we report in Table 5 the error of the EFNSR method as the step-size varies in time and space, for different values of ω. Note that for small perturbations (less than one) of the used frequency $\omega = \pi/10$, the errors are of the same order of magnitude. Instead, for big perturbations (greater than one), the error explodes or assumes high values, as expected. Finally, in Figure 8, left, and Table 6, we show that the behavior of the solution and the errors do not substantially change even using other functions with different frequencies as initial conditions. Specifically, we have fixed $u_1(x, 0) = cos(\pi x/5) + 1$, $u_2(x, 0) = cos(\pi x/10) + 1$, and $w(x, 0) = cos(3\pi x/10) + 1/10$, then computing the reference solution as before and using the same methods employed for Table 3.

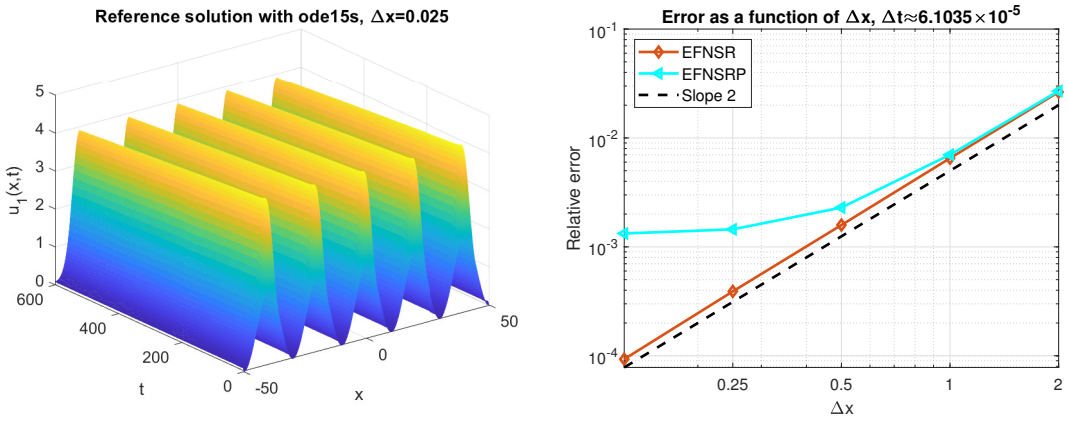

Figure 7: Component u_1 of the reference solution and trend of the errors by EFNSR and EFNSRP methods.

Table 5: Global relative error of the EFNSR method as Δx, Δt, and the frequency $\omega = (1+\delta)\pi/10$ vary.

Δx	Δt	$\delta = 0$	$\delta = 0.3$	$\delta = 0.6$	$\delta = 3$	$\delta = 9$
2	0.0625	2.6443e-02	1.8691e-02	1.2724e-02	1.9316e-01	-
$2/2$	$0.0625/2^2$	6.5252e-03	4.6495e-03	3.1205e-03	4.3600e-02	3.6674e-01
$2/2^2$	$0.0625/2^4$	1.5881e-03	1.1297e-03	7.6233e-04	1.0682e-02	7.8780e-02
$2/2^3$	$0.0625/2^6$	3.9040e-04	2.7672e-04	1.8754e-04	2.6613e-03	1.9473e-02

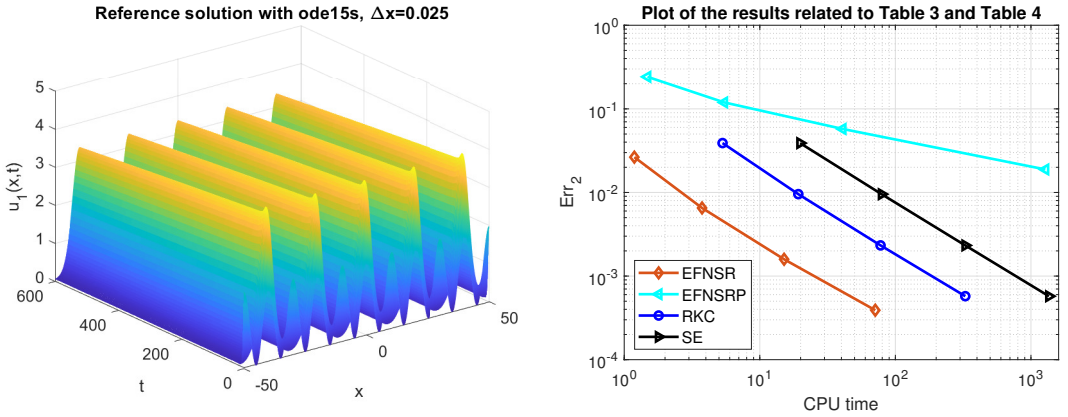

Figure 8: Component u_1 of the reference solution, fixing initial conditions as reported in the caption of Table 6, on the left, and efficiency plot related to results shown in Tables 3 and 4, on the right.

Table 6: Relative errors, setting $u_1(x,0) = cos(\pi x/5) + 1$, $u_2(x,0) = cos(\pi x/10) + 1$, and $w(x,0) = cos(3\pi x/10) + 1/10$.

Δx	Δt	EFNSR	EFNSRP	RKC	Δx	Δt	SE
2	0.0625	2.8341e-02	2.2415e-01	3.9028e-02	2	0.0025	3.9059e-02
$2/2$	$0.0625/2^2$	6.8296e-03	1.1495e-01	9.5447e-03	$2/2$	$0.0025/2^2$	9.5469e-03
$2/2^2$	$0.0625/2^4$	1.6649e-03	5.6145e-02	2.3278e-03	$2/2^2$	$0.0025/2^4$	2.3284e-03
$2/2^3$	$0.0625/2^6$	4.0977e-04	1.8480e-02	5.7437e-04	$2/2^3$	$0.0025/2^6$	5.7451e-04

7. Conclusions and future research

In this work, we built new NSFDs numerical methods for solving a system of three PDEs widely used in applications. These methods are semi-explicit, but nevertheless have excellent stability properties, and preserve all the most important characteristics of the analyzed model. They are very convenient and economical, as they are able to provide accurate results even for large values of the discretization steps. To construct such methods, we did not use the classic definition of NSFDs. In fact, inspired by the TASE technique, we have extended the definition of NSFDs. This allowed us not only to obtain methods with excellent stability properties, but also able to preserve the positivity of the exact solution. Furthermore, we demonstrated the link between NSFDs and EF. This is very useful, as from now on the NSFDs can also be applied to preserve the oscillating character, if present and known, of the exact solution of the treated model.

From this paper, an immediate research work that can be done concerns the proof of the fact that the derived NSFDs methods are able to preserve the metastability of the analyzed PDE system.

Acknowledgments
The authors are members of the GNCS group. This work is supported by GNCS-INDAM project and by the Italian Ministry of University and Research (MUR), through the PRIN 2020 project (No. 2020JLWP23) "Integrated Mathematical Approaches to Socio–Epidemiological Dynamics" (CUP: E15F21005420006) and the PRIN 2017 project (No. 2017JYCLSF) "Structure preserving approximation of evolutionary problems".
The authors are very grateful to the anonymous referees for their valuable remarks and comments on this paper.

References

[1] Anguelov, R., Lubuma, J.M.S., *Contributions to the mathematics of the nonstandard finite difference method and applications*. Numer. Methods Partial Differ. Equ., 17, 518-543, 2001.

[2] Bassenne, M., Fu, L., Mani, A., *Time-Accurate and highly-Stable Explicit operators for stiff differential equations*. J. Comput. Phys., 424, 109847, 2021.

[3] Berman, A., Plemmons, R.J., *Nonnegative Matrices in the Mathematical Sciences*. Academic Press, 1979.

[4] Bhatia, R., *Positive Definite Matrices*. Princeton Series in Applied Mathematics, 2007.

[5] Budroni, M.A., Pagano, G., Paternoster, B., D'Ambrosio, R., Conte, D., Ristori, S., Abou-Hassan, A., Rossi, F., *Synchronization scenarios induced by delayed communication in arrays of diffusively-coupled autonomous chemical oscillators*. Phys. Chem. Chem. Phys., 23(32), 17606-17615, 2021.

[6] Budroni, M.A., Pagano, G., Paternoster, B., D'Ambrosio, R., Conte, D., Ristori, S., Abou-Hassan, A., Rossi, F., *A Model for Coupled Belousov-Zhabotinsky Oscillators with Delay*. Conference Proceeding for 14th WCCM-ECCOMAS, DOI: 10.23967/wccm-eccomas.2020.026, 2021.

[7] Budroni, M.A., Torbensen, K., Ristori, S., Abou-Hassan, A., Rossi, F., *Membrane Structure Drives Synchronization Patterns in Arrays of Diffusively Coupled Self-Oscillating Droplets*. J. Phys. Chem. Lett., 11(6), 2014-2020, 2020.

[8] Bulai, I.M., Cavoretto, R., Chialva, B., Duma, D., Venturino, E., *Comparing disease-control policies for interacting wild populations*. Nonlinear Dyn., 79(3), 1881-1900, 2015.

[9] Calvo, M., Montijano, J. I., Rández, L., *A note on the stability of time–accurate and highly–stable explicit operators for stiff differential equations*. J. Comput. Phys., 436, 110316, 2021.

[10] Chapwanya, M., Lubuma, J.M.S., Mickens, R.E., *Positivity-preserving nonstandard finite difference schemes for cross-diffusion equations in biosciences*. Comput. Math. Appl., 68(9), 1071-1082, 2014.

[11] Conte, D., D'Ambrosio, R., Pagano, G., Paternoster, B., *Jacobian-dependent vs Jacobian-free discretizations for nonlinear differential problems*. Comput. Appl. Math., 39(3), 171, 2020.

[12] Conte, D., D'Ambrosio, R., Moccaldi, M., Paternoster, B., *Adapted explicit two-step peer methods*. J. Numer. Math., 27(2), 69-83, 2018.

[13] Conte, D., Mohammadi, F., Moradi, L., Paternoster, B., *Exponentially fitted two-step peer methods for oscillatory problems*. Comput. Appl. Math., 39(3), 174, 2020.

[14] Conte, D., Paternoster, B., Moradi, L., Mohammadi, F., *Construction of exponentially fitted explicit peer methods*. Int. J. Circuits Syst. Signal Process., 13, 501-506, 2019.

[15] Conte, D., Guarino, N., Pagano, G., Paternoster, B., *On the advantages of nonstandard finite differences discretizations for differential problems*. Numer. Anal. Appl., 25(3), 2022.

[16] D'Ambrosio, R., Esposito, E., Paternoster, B., *Exponentially fitted two-step Runge-Kutta methods: construction and parameter selection*. Appl. Math. Comput., 218(14), 7468-7480, 2012.

[17] D'Ambrosio, R., Paternoster, B., *Numerical solution of a diffusion problem by exponentially fitted finite difference methods*. SpringerPlus, 3, 425, 2014.

[18] D'Ambrosio, R., Paternoster, B., Santomauro, G., *Revised exponentially fitted Runge-Kutta-Nyström methods*. Appl. Math. Lett., 30, 56-60, 2014.

[19] D'Ambrosio, R., Moccaldi, M., Paternoster, B., *Adapted numerical methods for advection–reaction–diffusion problems generating periodic wavefronts*. Comput. Math. Appl., 74(5), 1029-1042, 2017.

[20] D'Ambrosio, R., Moccaldi, M., Paternoster, B., *Parameter estimation in IMEX-trigonometrically fitted methods for the numerical solution of reaction-diffusion problems*. Comput. Phys. Comm., 226, 55-66, 2018.

[21] Eigentler, L., Sherratt, J.A., *Metastability as a coexistence mechanism in a model for dryland vegetation patterns*. Bull. Math. Biol., 81, 2290-2322, 2019.

[22] Ganegoda, N., Gotz, T., Putra Wijaya, K., *An age-dependent model for dengue transmission: Analysis and comparison to field data*. Appl. Math. Comput., 388, 125538, 2021.

[23] Giamberardino, P.D., Iacoviello, D., Papa, F., Sinisgalli, S., *Dynamical evolution of COVID-19 in Italy with an evaluation of the size of the asymptomatic infective population*. IEEE J. Biomed., 25(4), 1326-1332, 2021.

[24] Gray, R.M., *Toeplitz and Circulant Matrices: A review*. Now Foundations and Trends, 2006.

[25] Higham, N.J., *Functions of Matrices: Theory and Computation*. SIAM, 2008.

[26] Hochbruck, M., Lubich, C., Selhofer, H., *Exponential integrators for large systems of differential equations*. SIAM J. Sci. Comput., 19(5), 1552-1574, 1998.

[27] Horn, R.A., Johnson, C.R., *Matrix Analysis*. Cambridge University Press, 2012.

[28] Ixaru, L.Gr., Vanden Berghe, G., *Exponential Fitting*. Springer, 2010.

[29] Ixaru, L.Gr., *Operations on oscillatory functions*. Comput. Phys. Commun., 105, 1-19, 1997.

[30] Ixaru, L.Gr., *Runge-Kutta methods with equation dependent coefficients*. Comput. Phys. Commun., 183(1), 63-69, 2012.

[31] Koroglu, C., *Exact and nonstandard finite difference schemes for the generalized KdV–Burgers equation*. Adv. Differ. Equ., 2020(1), 134, 2020.

[32] Koto, T., *IMEX Runge-Kutta schemes for reaction–diffusion equations*. J. Comput. Appl. Math., 215, 182-195, 2008.

[33] Kulkarni, D., Schmidt, D., Tsui, S.K., *Eigenvalues of tridiagonal pseudo-Toeplitz matrices*. Lin. Alg. Appl., 297(1-3), 63-80, 1999.

[34] Mickens, R.E., *Calculation of denominator functions for nonstandard finite difference schemes for differential equations satisfying a positivity condition*. Numer. Methods Partial Differ. Equ., 23(3), 672-691, 2007.

[35] Mickens, R.E., *Nonstandard finite difference schemes: Methodology and applications*. World Scientific, 2020.

[36] Niesen, J., Wright, W.M., *Algorithm 919: A Krylov subspace algorithm for evaluating the ψ-functions appearing in exponential integrators*. ACM Trans. Math. Softw., 38(3), 22, 2012.

[37] Plemmons, R.J., *M-matrix characterizations. I-nonsingular M-matrices*. Lin. Alg. Appl., 18(2), 175-188, 1977.

[38] Rafiq, M., Macías-Díaz, J.E., Raza, A., Ahmed, N., *Design of a nonlinear model for the propagation of COVID-19 and its efficient nonstandard computational implementation*. Appl. Math. Model., 89, 1835-1846, 2021.

[39] Salman, S.M., *A nonstandard finite difference scheme and optimal control for an HIV model with Beddington–DeAngelis incidence and cure rate*. Eur. Phys. J. Plus, 135(101), 808, 2020.

[40] Shaikh, T.S., Fayyaz, N., Ahmed, N., Shahid, N., Rafiq, M., Khan, I., Nisar, K.S., *Numerical study for epidemic model of hepatitis-B virus*. Eur. Phys. J. Plus, 136(4), 367, 2021.

[41] Ud Din, R., Shah, K., Ahmad, I., Abdeljawad, T., *Study of transmission dynamics of novel COVID-19 by using mathematical model*. Adv. Differ. Equ., 2020(11), 323, 2020.

[42] Van Daele, M., Vanden Berghe, G., *Geometric numerical integration by means of exponentially-fitted methods*. Appl. Numer. Math., 57, 415-435, 2007.

[43] Vanden Berghe, G., Ixaru, L.Gr., De Meyer, H., *Frequency determination and step-length control for exponentially-fitted Runge–Kutta methods*. J. Comput. Appl. Math., 132, 95-105, 2001.

[44] Vanden Berghe, G., Van Daele, M., Vande Vyver H., *Exponential fitted Runge–Kutta methods of collocation type: fixed or variable knot points*. J. Comput. Appl. Math., 159(2), 217-239, 2003.

[45] Verwer, J.G., Hundsdorfer, W.H., Sommeijer, B.P., *Convergence Properties of the Runge-Kutta Chebyshev Method*. Numer. Math., 57, 157-178, 1990.

[46] Viguerie, A., Veneziani, A., Lorenzo, G., Baroli, D., Aretz-Nellesen, N., Patton, A., Yankeelov, T.E., Reali, A., Hughes, T.J.R., Auricchio, F., *Diffusion–reaction compartmental models formulated in a continuum mechanics framework: application to COVID-19, mathematical analysis, and numerical study*. Comput. Mech., 66, 1131-1152, 2020.